euspen's 24th International Conference & Exhibition, Dublin, IE, June 2024
www.euspen.eu

Thermomechanical impact of the cutting edge microgeometry on the surface properties in turning of aluminium alloys

Thomas Junge[1], Thomas Mehner[2], Andreas Nestler[1], Andreas Schubert[1], Thomas Lampke[2]

[1]*Micromanufacturing Technology, Chemnitz University of Technology, Reichenhainer Str. 70, 09126 Chemnitz, Germany*
[2]*Materials and Surface Engineering, Chemnitz University of Technology, Erfenschlager Str. 73, 09125 Chemnitz, Germany*

thomas.junge@mb.tu-chemnitz.de

Abstract

In machining with tools exhibiting geometrically defined cutting edges their microgeometry has a significant influence on the surface properties. The process-adapted design of cutting edges enables a targeted modification of the thermomechanical load during machining as well as the resulting surface layer properties. In order to increase the fatigue strength of the machined parts and to enhance their application performance, low surface roughness values and strong compressive residual stresses are aspired. Hence, for the experimental investigations, the cutting edge geometry of cemented carbide indexable inserts is modified.The size and the orientation (form factor $K_S < 1$, $K_S > 1$) of the cutting edge rounding are changed by brushing. In the experimental investigations, the cutting speed (50 m/min and 550 m/min) and the depth of cut (0.4 mm and 0.8 mm) are varied, while the feed is kept constant. For an evaluation of the resulting thermal load in turning of the aluminium alloy EN AW-2017, the temperature is measured by a tool-workpiece thermocouple. Additionally, the components of the resultant force are recorded by a dynamometer.
The results show an enlargement of the tangential residual stresses with an increasing cutting edge radius due to rising temperatures in the cutting zone. Nevertheless, the selection of a low cutting speed and a high depth of cut combined with an appropriate orientation of the cutting edge rounding allows for strong compressive residual stresses. In-process monitoring of the cutting temperature and the force components enables a better comprehension of the thermomechanical impact. Although not all effects of the cutting edge geometry on the residual stresses can be explained by the results of the in-process measurements, the findings contribute to a tailored cutting edge design and selection of the machining parameters in regard to the desired surface properties.

Keywords: Aluminium, Cutting edge geometry, In-process monitoring, Surface properties, Turning

1. Introduction

The cutting edge microgeometry describes the transition area of the cutting edge from the rake face to the flank face. It can be modified by various processes (e.g. grinding, brushing, laser machining, etc.). The VDI Standard VDI/VDE 2654 Part 2 defines various cutting edge parameters for this purpose. Commonly, the cutting edge radius r_β is used for the characterisation of the edge rounding. The form factor K_S has been introduced to describe the orientation of the edge rounding towards the flank face ($K_S < 1$) or the rake face ($K_S > 1$). It is calculated by the division of the projected rounding on the rake face (S_γ) and flank face (S_α). Overall, the defined cutting edge design can have different purposes like the reduction of cutting edge chipping, the improvement of cutting edge stability and the enhancement of coating adhesion. However, modifying the cutting edge geometry is also accompanied by a change in machining conditions, in particular the thermomechanical load in the cutting zone. [1]

According to Bassett et al. [2], the cutting and feed forces increase significantly due to the intensification of friction and ploughing as a result of an increase in S_α as well as the average radius. In contrast, an orientation of the cutting edge rounding towards the rake face has hardly any influence on the forces. A high cutting edge radius especially for $K_S > 1$ can lead to the formation of a stagnation zone in the area of the cutting edge, similar to a sharp one, where the relative velocity between the tool and the workpiece material is temporarily equal to zero. This effect particularly applies for machining of aluminium where a stable built-up edge can influence the forces considerably [3]. Shen et al. [4] conclude that the resulting intensification of the ploughing effect can increase the absolute values of the compressive residual stresses in the material.

Bergmann [5] measured the temperatures inside the indexable insert with an embedded thermocouple during dry orthogonal turning of C45N, Ti6Al4V, and EN AW-2007. In contrast to C45N and Ti6Al4V, where the measured thermal load increased with a larger cutting edge radius ($K_S = 1$), there was no significant temperature rise (5%) measurable for the aluminium alloy. However, an empirically calculated temperature field showed that the temperature at the flank face rises with an increase in S_α. According to the FEM model by Bergmann et al. [6] for the simulation of the thermomechanical during machining, the increased friction in the transition area to the flank face is the main reason for that.

In milling, Denkena et al. [7] investigated the influence of the cutting edge radius on the resulting residual stresses of the aluminium alloy EN AW-7449 in milling. On the one hand, they observed stronger compressive residual stresses beneath the surface with an increasing cutting edge radius. On the other hand, the tensile residual stresses at the surface rose simultaneously.

Considering the influence of the cutting edge microgeometry on the surface roughness, inconsistent findings can be observed. In this regard, the ratio of undeformed chip thickness to cutting edge radius must be taken into account. The smaller the ratio, the higher the ploughing effect, which increases the material

flow along the flank face and thus could lead to a deterioration of the surface roughness. [1]

The state of the art in science and technology shows that the modification of the cutting edge microgeometry can change the thermomechanical load and therefore the resulting surface properties during machining. Nevertheless, the impact is strongly related to the material properties, e.g. the thermal conductivity and strength [6]. In this context, there has been no comprehensive experimental investigation in machining of aluminium alloys up to now. Therefore, the object of this study is the characterisation of the thermomechanical impact during machining of EN AW-2017 with different cutting edge microgeometries and its influence on the surface properties with special emphasis on the residual stresses. It is of high interest if the modification of the cutting edge microgeometry can contribute to the enhancement of the fatigue strength of finish machined aluminium parts.

2. Materials and Methods

2.1. Specimens and cutting tools

In the experimental investigations, cylindrical specimens of the aluminium alloy EN AW-2017 (T4) with a total length of 80 mm were used. The specimens were stepped and had a diameter of 28 mm for a length of 60 mm. For the remaining part of the length, the diameter amounted to 25 mm. The side with the smaller diameter was utilised for clamping applying a dead-length collet chuck.

In the finish machining experiments, uncoated cemented carbide indexable inserts of the type CCMT 09T304 were used. They were characterised by a tool included angle of 80°, a clearance angle of 7°, a rake angle of 0°, and a corner radius r_ε of 0.4 mm. In combination with the tool holder used, the nominal tool cutting edge angle of the major cutting edge was 95°. After grinding, the cemented carbide indexable inserts were characterised by a cutting edge rounding r_β of 7 µm (tool type 1) with a form factor K_S of 0.8. For a variation of the cutting edge microgeometry the tools were modified by brushing. Afterwards the cutting edges were measured by an optical coordinate measuring machine (Bruker alicona µCMM). The cutting edge radius and form factor were evaluated by the Alicona Edge Master Module by extracting 50 orthogonal profiles each in the area of the tool corner and the major cutting edge. Table 1 shows the average values of four tools with the same cutting edge characteristics and their mean absolute deviations.

Table 1 Measured cutting edge radius r_β and form factor K_S of the applied cutting tools and their mean absolute deviations

Tool type	Cutting edge radius r_β / µm	Form factor K_S
1	7.3 ± 0.1	0.80 ± 0.02
2	14.4 ± 1.5	0.73 ± 0.06
3	28.6 ± 3.2	0.98 ± 0.04
4	15.6 ± 1.2	1.75 ± 0.04

Comparing the orientation of the cutting edge rounding of tool type 1 to 3, it can be seen that the reproducibility of the same form factor is difficult to achieve for different cutting edge roundings. The rise of the mean absolute deviation of r_β from tools type 1 to type 3 results from the brushing process and can be explained by the increasing deviation between r_β in the area of the corner radius and the main cutting edge. Figure 1 shows a modified cutting edge microgeometry in comparison to a tool after grinding captured by 3D laser scanning microscopy using a Keyence microscope type VK-9700.

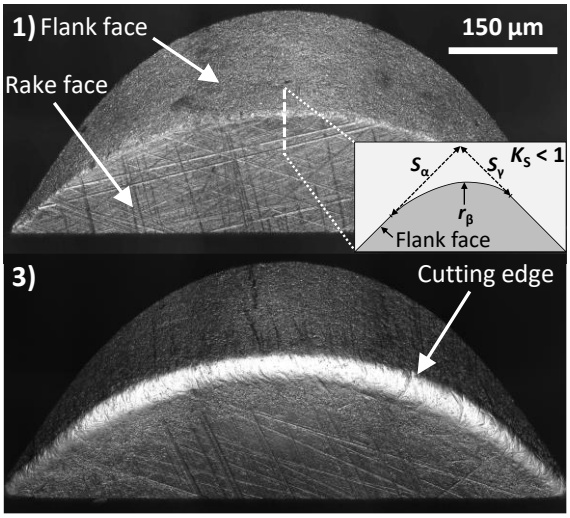

Figure 1. Microscope images of the cutting edges of tools type 1 and type 3 in the area of the tool corner as well as a schematic depiction of a form factor $K_S < 1$ ($S_\alpha > S_\gamma$)

2.2. Measurement principles and implementation

For the acquisition of the mechanical load the tool holder was mounted on a three-axis dynamometer type 9257 A (Kistler), which was connected to a charge amplifier type 5070 A (Kistler). Therefore, the cutting force F_c, the feed force F_f, and the passive force F_p could be recorded separately during machining.

The evaluation of the thermal load close to its point of origin was realised by the application of a tool-workpiece thermocouple. It is similar to a conventional thermocouple except for the fact that workpiece and tool form a natural thermocouple. The measured thermoelectric voltage corresponds to the average temperature at the interface of the tool and the specimen [8]. The complete setup of the tool-workpiece thermocouple and its integration into the lathe are described and visualised in detail in [9].

2.3. Machining experiments

The experimental investigations were conducted on a precision lathe of the type SPINNER PD 32. For pre-machining of the specimens, an indexable insert comprising a CVD diamond tip was used. The applied machining parameters were constant (feed f = 0.1 mm, depth of cut a_p = 0.1 mm, and cutting speed v_c = 150 m/min). To avoid a significant heating of the specimen, it was cooled applying a cold-air nozzle. After pre-machining, the specimens had a diameter of 27.8 mm.

During finish machining experiments, the tools listed in Table 1 were used. The thermal load was altered by choosing cutting speeds of 50 m/min and 550 m/min due to the direct correlation between the cutting speed and the process temperature. Furthermore, a change in the cutting edge length in contact with the workpiece material was obtained by selecting two different depths of cut of 0.4 mm and 0.8 mm. The feed was kept constant at 0.04 mm. For each combination of cutting speed and depth of cut, two specimens were machined with one tool. All experiments were performed with emulsion flood cooling in an air-conditioned laboratory.

2.4. Evaluation of surface properties

The geometrical properties of the machined surfaces were measured using a stylus instrument type Mahr LD 120. The stylus was characterised by a spherical radius of 2 µm and an included angle of 90°. After finish machining, the surface roughness of all specimens was measured in the direction of feed motion. Three measurements, each with an evaluation length of 4 mm, were taken at different positions along the circumference at the

beginning and at the end of the specimen. Filtering of the profiles was done in accordance with DIN EN ISO 21920-3.

Residual stresses σ were measured on the specimen surface by X-ray diffraction (XRD) using the $\sin^2\psi$ method. One specimen was measured for each parameter set. A diffractometer D8 Discover (Bruker) with a Co anode (parameters 35 kV, 40 mA), a 0.5 mm pinhole aperture, and a 1D detector LYNXEYE XE-T has been utilised. The tilt angles ψ were selected in such a way that their spacing on the $\sin^2\psi$ scale is 0.1 (between 0 and 0.8 – both in positive and negative tilt direction). Rotation angles φ 0°, 45°, and 90° were used. The measurements were performed using the {311} peak of Al with the lattice-specific elastic constants Young's modulus $E^{\{311\}}$ = 69.3 GPa and Poisson's ratio $\nu^{\{311\}}$ = 0.35 [10].

3. Results and discussion

3.1. Thermomechanical process conditions

In a first step, the thermomechanical impact of the form factor $K_S < 1$ (tool type 2) and $K_S > 1$ (tool type 4) was compared for similar cutting edge radii. Regarding the tool-workpiece interface temperature no significant change was visible as the highest temperature difference amounted to only 11.6 K (v_c = 550 m/min, a_p = 0.4 mm). The same result could be obtained for the measurement of the components of the resultant force, where the maximum force difference due to a higher form factor amounted to 1.5 N for F_c, 1.8 N for F_f, and 1 N for F_p over all experimental tests. Consequently, the variation of the form factor in the range from 0.7 to 1.8 had no measurable influence on the thermomechanical load.

In a second step, the effect of an increasing cutting edge radius on the thermomechanical impact was analysed for similar form factors. Figure 2 shows the tool-workpiece interface temperature T for tools of type 1 – 3 in dependence of cutting speed and depth of cut. The diagram displays the mean values of the measurements calculated from two equivalent tests and the standard deviations over the course of the measurements.

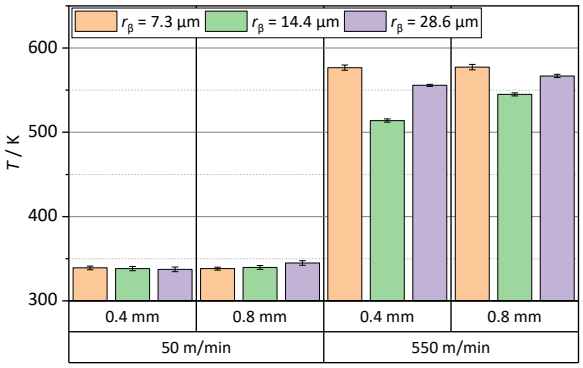

Figure 2. Influence of the cutting edge radius r_β on the tool-workpiece interface temperature for different v_c and a_p

Since the majority of the mechanical energy supplied to the cutting process is converted into thermal energy, there is a significant growth of the interface temperature with increasing cutting speed. On the one hand, there is no temperature change visible in regard to different cutting edge radii for the low cutting speed. On the other hand, high cutting speeds lead to lower temperatures for tools of type 2 and type 3 in comparison to tool type 1, but there is no clear tendency concerning the cutting edge radius.

Figure 3 illustrates the average values of the components of the resultant force calculated from two similar experiments. The error bars represent the mean standard deviation over the course of the measurements.

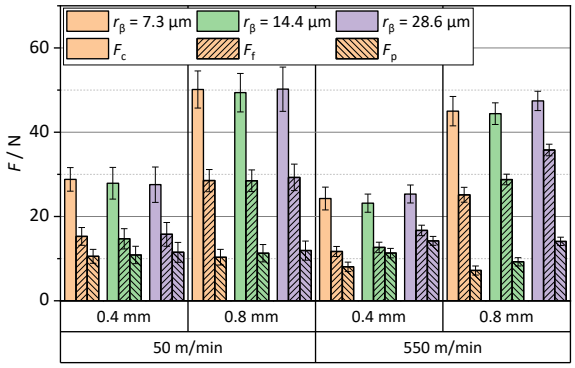

Figure 3. Influence of the cutting edge radius r_β on the components of the resultant force for different v_c and a_p

The increase in depth of cut leads to an enlargement of the cross-sectional area of the undeformed chip. Hence, the work required for elastic and plastic deformation of the material increases and enlarges the cutting and feed forces. However, with a higher cutting speed the cutting force slightly decreases due to the material strength reduction resulting from higher temperatures. For v_c = 550 m/min the feed and passive forces rise steadily with an enlargement of the cutting edge radius. This force enhancement could result from increased material flow towards the flank face (ploughing) and intensified squeezing of the material in the shear zone. Surprisingly, this mechanical impact of the cutting edge radius is not visible for lower cutting speeds. This behaviour could be attributed to increased built-up edge (BUE) formation at low temperatures, illustrated in Figure 4.

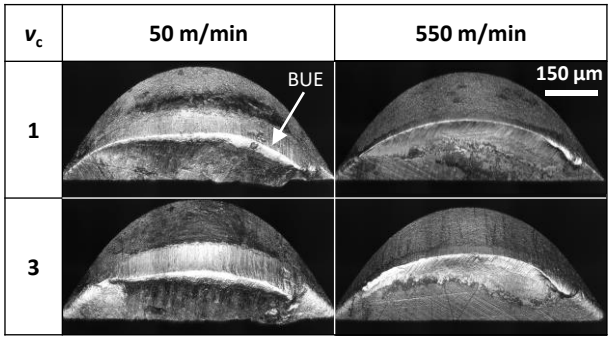

Figure 4. Microscope images of the cutting edges of tools of type 1 and type 3 in the area of the tool corner after machining for a_p = 0.4 mm

Due to strain hardening the deposited aluminium material is harder than the specimen material and thus it takes over the function of the cutting edge. The temporarily changed cutting edge microgeometry has a different cutting edge radius and a higher rake angle of up to 25°. Therefore, the BUE alters the material flow and counteracts the force enhancing effect by an increased cutting edge radius.

3.2. Surface properties

Independent of the cutting edge radius, the surface roughness values varied between 1.3 µm – 2.1 µm for *Rz* and 0.16 µm – 0.34 µm for *Ra* across all experimental tests. However, no consistent trend or significant change in surface roughness was observed that could be explained by the modification of the cutting edge rounding. Therefore, it is not considered in detail in this study.

Different cutting edge microgeometries and machining parameters change the residual stress distribution in axial and tangential direction (Figure 5). These stress modifications depend on the components of the resultant force and the cutting temperature.

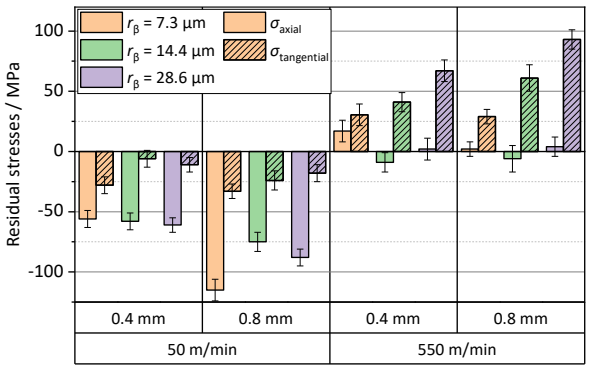

Figure 5. Influence of the cutting edge radius r_β on on the residual stresses in the axial and the tangential direction for different v_c and a_p

For low cutting speeds compressive residual stresses are dominant due to the overall minor temperature changes of the specimens. They become even stronger by an increase of the cutting and feed forces as a result of higher plastic deformation. In contrast, this mechanical impact is not visible for the higher cutting speed as the thermal influence increases.

In reference to [2] and [6] a higher cutting edge radius in combination with a form factor $K_S \leq 1$ leads to an increase in the contact surface between the tool and the specimen material in the area of the flank face. Furthermore, the rise of the sliding friction work between tool and workpiece contributes to a rise of the frictional heat. Finally, the enlarged contact surface in the tertiary shear zone favours the heat transfer into the specimen and therefore leads to an increase in the residual stresses in the tangential direction with rising cutting edge radius (see Figure 5). Since the cutting speed is significantly higher than the feed velocity, this effect is not observed in the axial direction, where no significant influence of the cutting edge rounding is evident. The described local increase of the thermal load cannot be seen in Figure 2 because the tool-workpiece thermocouple only measures the average temperature of the contact surface between the tool and the specimen. Since the tool-specimen contact surface on the rake face is larger than the contact surface in the area of the flank face a temperature change in the tertiary shear zone can hardly be measured.

Despite there were no significant measurable differences of the thermomechanical load during machining with tools comprising different orientations of the cutting edge rounding, tangential residual stresses changed (Figure 6).

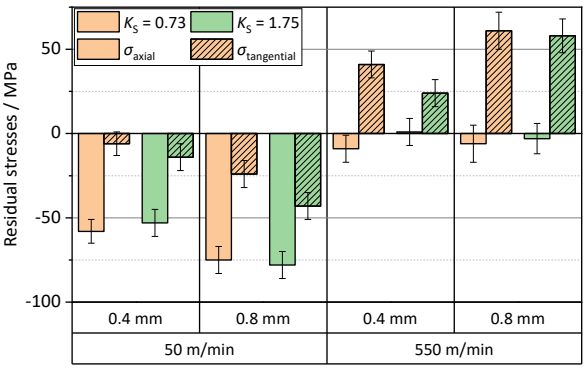

Figure 6. Influence of the form factor K_S on on the residual stresses in the axial and the tangential direction for different v_c and a_p

With the enlargement of the form factor tangential residual stresses decrease. The more the cutting edge rounding is orientated towards the rake face ($K_S > 1$), the smaller the contact surface between tool and specimen. This leads to a reduced heat input into the specimen resulting in enhanced compressive or lower tensile residual stresses in the tangential direction, respectively. Additionally, the surface roughness values for *Rz* were reduced slightly in experimental tests by up to 0.4 µm.

5. Summary and conclusions

Different cutting edge geometries are evaluated concerning their thermomechanical influence on the surface properties in turning of EN AW-2017. The experimental findings reveal a significant dependency from the cutting speed. Low process temperatures lead to increased built-up edge formation, that counteracts the force enhancing effect of an increased cutting edge rounding. However, the enlargement of the mechanical load for higher cutting speeds shows no clear effect on the residual stresses as its influence is suppressed due to the more dominant thermal influence. Overall, the results confirm that low temperatures favour the generation of compressive residual stresses. In this context, the modification of the residual stresses by the changed cutting speed could be explained as a result of the global thermomechanical load. However, the local thermal impact of the cutting edge geometry cannot be depicted by the tool-workpiece thermocouple as the increase of the contact surface between the tool and the specimen due to a larger cutting edge radius is too small in relation to the overall size of the contact surface.

It can be assumed that the enlarged heat transfer into the specimen leads to a rise of tangential residual stresses. Consequently, it is not recommended to apply a tool with a large cutting edge radius and a form factor $K_S \leq 1$ for machining of aluminium parts with a desired high fatigue strength. Nevertheless, compressive residual stresses can be obtained by applying a low cutting speed and a higher depth of cut. In terms of tool design, a slight reinforcement of the compressive residual stresses in the tangential direction can be achieved by a form factor $K_S > 1$.

Further investigations should examine in more detail the local heat input in the tertiary shear zone by the application of FEM simulations leading to better comprehension of the thermomechanical impact of the cutting edge microgeometry.

Acknowledgements

The scientific work has been supported by the DFG within the research priority programme SPP 2086 (SCHU 1484/26-2, LA 1274/49-2) grant number 401805994. The authors thank the DFG for this funding and intensive technical support.

References

[1] Denkena B and Biermann D 2014 Cutting edge geometries *CIRP Annals* **63**(2) 631-653

[2] Bassett E et al. 2012 On the honed cutting edge and its side effects during orthogonal turning operations of AISI1045 with coated WC-Co inserts *CIRP J. Manuf. Sci. Technol.* **5**(2) 108-126

[3] Waldorf D J et al. 1999 An Evaluation of Ploughing Models for Orthogonal Machining ASME *J. Manuf. Sci. Eng.* **121**(4) 550-558

[4] Shen Q et al. 2018 Effects of Cutting Edge Microgeometry on Residual Stress in Orthogonal Cutting of Inconel 718 by FEM *Materials* **11**(6) 1015

[5] Bergmann B 2017 Grundlagen zur Auslegung von Schneidkantenverrundungen (PhD) Hannover: *TEWISS* **IFW 9/2017**

[6] Bergmann B et al. 2021 FE-Simulation Based Design of Wear-Optimized Cutting Edge *Roundings J. Manuf. Mater. Process.* **5**(4) 126

[7] Denkena B et al. 2008 Machining induced residual stress in structural aluminum parts *Prod. Eng. Res. Devel.* **2** 247–253

[8] Stephenson D A 1993 Tool-Work Thermocouple Temperature Measurements: Theory and Implementation Issues ASME *J. Ind. Eng. Int.* **115** 432-437

[9] Junge T et al. 2024 Methodology for soft-sensor design and in-process surface conditioning in turning of aluminum alloys *Prod. Eng. Res. Devel.* **18** 267-287

[10] Eigenmann B and Macherauch E 1996 Röntgenographische Untersuchung von Spannungszuständen in Werkstoffen (Teil 3) *Mater. Werkst.* **27** 426-437